

Flexural behaviour of fibre reinforced geopolymer concrete composite beams

Vijai K^{*1}, Kumutha R^{1a} and Vishnuram B.G.^{2b}

¹Department of Civil Engineering, Sethu Institute of Technology, Kariapatti, Tamilnadu, India

²P.S.R. Engineering College, Sivakasi, Tamilnadu, India

(Received October 15, 2014, Revised January 5, 2015, Accepted January 7, 2015)

Abstract. An experimental investigation on the behaviour of geopolymer composite concrete beams reinforced with conventional steel bars and various types of fibres namely steel, polypropylene and glass in different volume fractions under flexural loading is presented in this paper. The cross sectional dimensions and the span of the beams were same for all the beams. The first crack load, ultimate load and the load-deflection response at various stages of loading were evaluated experimentally. The details of the finite element analysis using "ANSYS 10.0" program to predict the load-deflection behavior of geopolymer composite reinforced concrete beams on significant stages of loading are also presented. Nonlinear finite element analysis has been performed and a comparison between the results obtained from finite element analysis (FEA) and experiments were made. Analytical results obtained using ANSYS were also compared with the calculations based on theory and presented.

Keywords: geopolymer; steel fibre; polypropylene fibre; glass fibre; volume fraction; ultimate load; finite element analysis.

1. Introduction

Cement concrete is one of the most commonly used construction materials. Usually concrete is produced by using the Ordinary Portland Cement as the binder. However, the manufacturing process of Portland Cement is an energy intensive process during which a very large amount of green house gases are being released to the atmosphere (Roy 1999). Production of one ton of Portland cement requires about 2.8 tons of raw materials that includes fuel and other materials and hence it is well known that the production of cement drains momentous amount of natural resources. As a result of calcination of lime, manufacturing of one ton of cement generates about one ton of carbon dioxide.

Nowadays, there is a big concern about the development of alternative materials to Portland cement. Therefore, there are efforts to develop the other form of cementitious materials for producing concrete. In order to address the above said issues, several new materials were projected to replace the function of cement in concrete. Fly ash, Rice husk ash, silica fume and Ground

*Corresponding author, Professor, E-mail : vijai_me@yahoo.co.in

^aProfessor, E-mail : kumuthar@yahoo.co.in

^bProfessor, E-mail : dr.bgvishnuram@gmail.com

Granulated Blast furnace Slag are some of the examples of cement replacement materials that are commonly used. The binder product that resulted from pozzolanic reaction between cement replacement materials and hydration paste has significantly improved conventional concrete properties. However, these materials can only replace up to certain percentages of portion of cement in concrete. High volume fly ash concrete has been developed by Malhotra (2002a,b) that utilized fly ash to replace cement up to 60% without reducing the performance of concrete. Replacement of cement above 60% would not provide any improvement to the performance of concrete, therefore new binder material that could entirely replace cement in concrete is indispensable to create better and more environmentally friendly concrete. In 1978, a new material was introduced by Davidovits (1999), which can be used as an alternative binder to cement. This material was named as geopolymer for its reaction between alkaline liquid and geological based source material.

Vijaya Rangan *et al.* (2006) carried out extensive studies on fly ash-based geopolymer concrete utilizing low calcium fly ash as the source material. The prominent factors that control the properties of the fresh concrete and the hardened concrete have been identified. From the experimental investigations it has been found that fly ash-based geopolymer concrete has outstanding compressive strength and is appropriate for structural applications. The elastic properties of hardened concrete and the strength and behaviour of reinforced structural members are comparable to those of Portland cement concrete. Hence it is concluded that, the design provisions enclosed in the current codes and standards can be used to design reinforced fly ash-based geopolymer concrete structural members. The fly ash-based geopolymer concrete also shows excellent resistance to sulfate attack, undergoes low creep, and suffers very little drying shrinkage (Wallah and Rangan 2006). The applications of geopolymer concrete in the construction industry and the economic worthiness of geopolymer concrete were also highlighted by Vijaya Rangan (2008). Anurag Mishra *et al.* (2008) studied the effect of concentration of NaOH and curing time on fly ash based geopolymer concrete and the results of the investigation indicated that, there was an increase in compressive strength with increase in NaOH concentration. The compressive strength also increased with increase in curing time, but it was found that the increase in compressive strength was not significant after 48 hours of curing time. In another investigation, Siva Konda Reddy *et al.* (2010) prepared geopolymer concrete from low lime based fly-ash and found that the workability of geopolymer concrete gets reduced with higher concentrations of sodium hydroxide solution which resulted in a higher compressive strength. Amol A Patil *et al.* (2014) reported an experimental work conducted to investigate the effect of curing conditions such as ambient curing and hot curing on the compressive strength of geopolymer concrete and the results indicated that the increase in the strength is considerable in respect of ambient curing as compared to that of hot curing condition.

Experimental investigations were reported by Anuar *et al.* (2011) on geopolymer concrete using waste paper sludge ash as the source material and by incorporating recycled concrete aggregates. It was concluded that the compressive strength of waste paper sludge ash based geopolymer concrete incorporating recycled concrete aggregates increases by increasing the molarities of sodium hydroxide. Monita Olivia and Hamid R. Nikraz (2011) investigated the development of strength, water absorption and water permeability of low calcium fly ash geopolymer concrete by varying the water to binder ratio, aggregate to binder ratio, aggregate grading, and alkaline to fly ash ratio. Test results indicated that the strength of fly ash geopolymer concrete was increased by reducing the water to binder and aggregate to binder ratios and the water absorption of low calcium fly ash geopolymer was improved by decreasing the water to binder ratio, increasing the fly ash content, and using a well-graded aggregate. It was also observed that there was no major change in water

permeability coefficient for the geopolymer concrete with different parameters. The test data indicates that a good quality low calcium fly ash geopolymer concrete can be produced with appropriate parameterisation and mix design. Monita Olivia and Hamid R. Nikraz (2011) have also investigated the water penetrability properties, namely water absorption, volume of permeable voids, permeability and sorptivity of low calcium fly ash geopolymer concrete. Test results indicated that geopolymer concrete has low water absorption, volume of permeable voids and sorptivity. It was also concluded that the geopolymer concrete could be classified as a concrete with an average quality in keeping with water permeability value. Moreover, a low water to binder ratio and a well-graded aggregate are considered to be some of the significant factors to achieve low water penetrability of geopolymer concrete.

The results of an experimental study on the durability aspects of fly ash based Geopolymer concretes exposed to 10% sulphuric acid solutions for up to 8 weeks have been presented by X.J.Song *et al* (2005). The results confirmed that geopolymer concrete is highly opposed to sulphuric acid in terms of a very low mass loss, less than 3%. It was also observed that, geopolymer cubes were structurally undamaged and still had substantial load capacity even though the entire section had been neutralized by sulphuric acid. Hence, significant research works on fly ash based geopolymer concrete manufactured from fly ash in combination with sodium silicate and sodium hydroxide solution has been carried out by several researchers and they have reported higher strength and better durability of geopolymer concrete than Portland cement concrete. But, in spite of enormous researches on various aspects of geopolymer concrete, current applications of geopolymer concrete are affected by its curing method. The necessity of elevated temperature in its maturing period is supplied with electric equipment that could produce heat or hot steam. This method would avoid the geopolymer concrete to be applied in a cast in situ concrete work. Therefore this research is also paying attention on the utilization of ambient temperature to cure the geopolymer concrete by introducing geopolymer concrete composites.

Also the concept of addition of fibres as internal reinforcement in concrete is not new. By the 1960s, steel, glass (GFRC), and synthetic fibres such as polypropylene fibres were used in concrete, and research into new FRCs continues today. Some types of fibres produce greater impact, abrasion, and shatter resistance in concrete. Concerning the structural applications, fibre concrete possesses many advantages compared to the traditional structural concrete. Ganesan *et al.* (2013) compared the engineering properties of geopolymer concrete and steel fibre reinforced geopolymer concrete (SFRGPC) with different percentages of steel fibres. In general, the addition of fibres improved the mechanical properties of geopolymer concrete. An attempt was also made to find the relation between the various engineering properties with the percentage of fibres added. Although a lot of research has been carried out on geopolymer concrete on the various mechanical properties such as compressive strength, tensile strength and flexural strength, relatively less work has been performed on fibre reinforced geopolymer concrete to examine the effects of addition of fibres on the structural performance. The ductility improvement of geopolymer concrete is a crucial factor in concrete science and hence the objective of this research is to provide data and to gain insight into the behaviour of fibre reinforced geopolymer concrete composites. In addition to that, the information on the flexural behavior of fibre added geopolymer reinforced concrete beams is not found in the past literatures. And yet this information is vital for the use of fibre reinforced geopolymer concrete for structural applications. Therefore, extensive experimental and analytical investigations were carried out, to study the flexural behavior of plain and fibre added geopolymer composite reinforced concrete beams.

2. Experimental program

2.1 Parameters of study

The following parameters were considered in this experimental investigation:

- (a) Types of fibres: Steel fibre, Polypropylene fibre and Glass fibre
- (b) Volume fraction of fibres: Steel fibre - 0% , 0.25% , 0.5% and 0.75% ; Polypropylene fibre - 0% , 0.1% , 0.2% and 0.3% ; Glass fibre - 0% , 0.01% , 0.02% and 0.03%

2.2 Materials used

Fly ash: Class F dry fly ash conforming to IS 3812-2003 obtained from Mettur thermal power station of Tamilnadu from southern part of India was made use of in the casting of the specimens. Table 1 gives the chemical composition of fly ash used in this experimental investigation. Cement: Ordinary Portland Cement (OPC) conforming to I: 8112 – 1989, having a specific gravity of 3.15 was made use of, in the casting of the specimens. Table 2 gives the properties of cement used. Fine Aggregate: Locally available river sand having a bulk density of 1693 kg / m³, fineness modulus of 2.75, specific gravity of 2.81 and conforming to grading zone-III as per IS: 383 - 1970 was used. Coarse Aggregate: Crushed granite coarse aggregates of 19 mm maximum size having a fineness modulus of 6.64 and specific gravity of 2.73 were used. Bulk density of the coarse aggregate used is 1527 kg / m³. Sodium Hydroxide: Sodium hydroxide solids in the form of flakes with 97% purity was used in the preparation of alkaline activator. Sodium Silicate: Sodium silicate in the form of solution was used in the preparation of alkaline activator. The chemical composition of Sodium silicate solution supplied by the manufacturers is as follows: 14.7%, of Na₂O, 29.4% of SiO₂ and 55.9% of water by mass. Super plasticiser: To achieve workability of fresh geopolymer concrete, Sulphonated naphthalene polymer based super plasticizer Conplast SP430 in the form of a brown liquid instantly dispersible in water, was used in all the mixtures. Water: Distilled water was used for the preparation of sodium hydroxide solution and for extra water added to achieve workability. Fibres: Three types of fibres have been used in this investigation and the fibres used are shown in Figs.1(a) –(c): (1) Hooked-end steel fibres made with low carbon steel having a length of 35mm and a diameter of 0.5mm thus giving an aspect ratio of 70 were used. These fibres have a density of 7850 kg/m³, Modulus of elasticity of 2×10^5 MPa and Yield strength



(a) Steel fibres

(b) Polypropylene fibres

(c) Glass fibres

Fig. 1 Fibres Used

Table 1 Chemical composition of fly ash

Oxides	Mettur Fly ash	Requirements as per IS 3812-2003
SiO ₂	69.31%	SiO ₂ >35% Total - >70%
Al ₂ O ₃	12.26%	
Fe ₂ O ₃	3.14%	
CaO	1.92%	-
Na ₂ O	0.11%	Na ₂ O + K ₂ O <1.5%
K ₂ O	0.57%	
MgO	1.60%	<5%
LOI	5.48%	<12%

Table 2 Properties of cement

Description of test	Test results	Requirements of IS:8112 - 1989
Initial setting time	70 minutes	Min. 30 minutes
Final setting time	295 minutes	Max. 600 minutes
Compressive strength of cement mortar cubes at:		
3 days	24.69 MPa	23 MPa
7 days	34.65 MPa	33 MPa
28 days	46.58 MPa	43 MPa

of 650 MPa. (2) Polypropylene fibres having a length of 6mm and a diameter of 0.02 mm were used. These fibres have a density of 910kg/m³, Modulus of elasticity of 3500 MPa and yield strength of 550 MPa. (3) Alkali resistant glass fibres having a length of 6mm and a diameter of 0.014 mm were used. These fibres have a density of 2680kg/m³, Modulus of elasticity of 72000 MPa and Yield strength of 3400 MPa.

2.3. Preparation of test specimens

In this investigation, totally ten reinforced concrete beams were cast with and without fibres. Three beams were cast with steel fibres in volume fractions of 0.25%, 0.5% and 0.75%. Another three beams were cast with polypropylene fibres with volume fractions of 0.1%, 0.2% and 0.3%. Three more beams containing glass fibres with volume fractions of 0.01%, 0.02% and 0.03% were cast. The cross sectional dimensions and the span of the beams were fixed same for all the ten beams. The dimensions of the beams were 100 mm × 150 mm × 1000 mm. All the beams were reinforced using two numbers of 8 mm diameter tor steel bars at the bottom face that serves as the main reinforcement. The yield strength of the main reinforcement was found to be 547 MPa. Two numbers of 8mm diameter tor steel bars were used as hanger bars at the top and 6mm diameter mild steel stirrups @ 100 mm c/c spacing were provided as shear reinforcement as shown in Fig. 2.

In the mix design of geopolymer concrete, the coarse and fine aggregates together are

considered as 77% by mass. Fine aggregate was taken as 30% of the total aggregates. Assuming the average density of fly ash-based geopolymer concrete as 2400 kg/m^3 , the combined mass of alkaline liquid and fly ash was arrived. The ratio between the alkaline liquid and the fly ash is assumed as 0.4 and the mass of alkaline liquid was found out. Similarly, the ratio of sodium silicate solution to sodium hydroxide solution is fixed as 2.5, through which the mass of sodium hydroxide and sodium silicate solutions is found out. Extra water and super plasticizer Conplast SP 430 were added to the mix by 10% and 3% by weight of fly ash respectively to achieve a workable concrete. To avoid delayed setting and heat curing, 10% fly ash was replaced by OPC and the mix is designated as GPCC. The details of mix proportions adopted for the casting of geopolymer composite RC beams are given in Table 3. For the casting of beams wooden moulds were used. The concrete was compacted well by filling the beam moulds in 3 layers, each of approximately 50mm deep, ramming heavily and vibrating the specimens using a needle vibrator till the slurry appears at surface of the specimen. The side forms of moulds were stripped after 24 hours and then these beams were cured for 28 days in ambient curing at room temperature. For each mix, three cubes of size $150 \text{ mm} \times 150 \text{ mm} \times 150 \text{ mm}$ and three prisms of size $100 \times 100 \times 500 \text{ mm}$ were also cast as companion specimens to find out the compressive strength and flexural strength respectively.

2.4 Instrumentation and testing procedure

All the beams were tested in a Universal Testing Machine of 1000 kN capacity. Beams were simply supported over a span of 900 mm. The load was distributed as two line loads kept 150 mm apart symmetrical to centerline of beam on the top face such that the distance between the two loading lines is 300 mm and the distance between the loading lines and the nearest support is also 300 mm. Loading arrangement for beam specimens is shown in Fig. 3. The loading arrangement and instrumentation were same for all the beams. Deflection at the centre line of the beam was measured for every 0.5 kN increment of load using a dial gauge fitted at the centre.

3. Results and discussion

3.1 First crack load and ultimate load

The results of the first crack load and ultimate load for all the beams are summarised in Table 4. The results of the companion specimens that were cast along with the beams are also presented. From the test results it can be seen that the addition of fibres increases the load carrying capacity for all the beams. For steel fibres, the first crack load and the ultimate load increased as the volume fraction increases.

The gain in ultimate load carrying capacity is more significant in the case of SFRGPCC beams due to the addition of fibres. When compared to GPCC beams, the ultimate load increases by 18%, 36% and 47% for 0.25%, 0.5% and 0.75% of steel fibres respectively. The increase in load carrying capacities may be due to the sufficient bridging action of steel fibres across the cracks. In case of polypropylene fibres the first crack load increases as the volume fraction of fibres increases. But due to the addition of polypropylene fibres, the increase in ultimate load is very

marginal as compared to control GPCC beam. The increase in load carrying capacity is only in the order of 2% even for a volume fraction of 0.3%. A similar trend was observed for GFRGPCC beams also. The increase in ultimate load was not that much significant when compared to control GPCC beam. The ultimate load increases by only about 6%, 2% and 6% for 0.01%, 0.02% and 0.03% of glass fibres respectively.

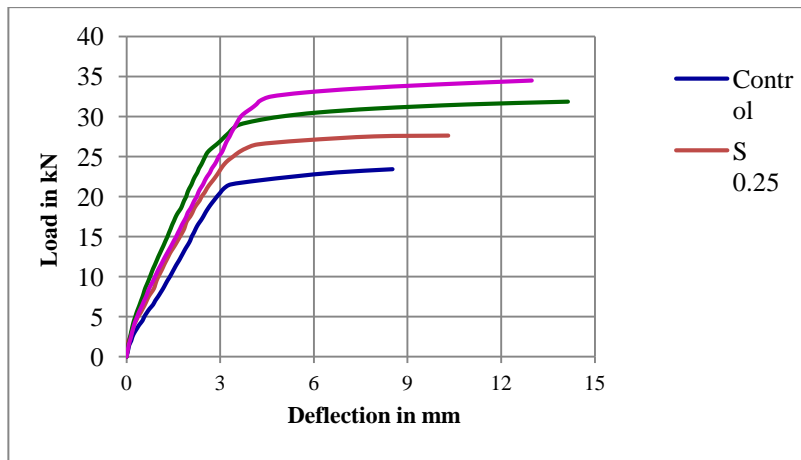
3.2 Ductility factor

An attempt was made in the present investigation to obtain the ductility factor for all the beams tested. The ductility factor is defined as the ratio of the ultimate deflection (δ_u) to the deflection at yield (δ_y). The values of the ductility factor for all the beams are presented in Table 5.

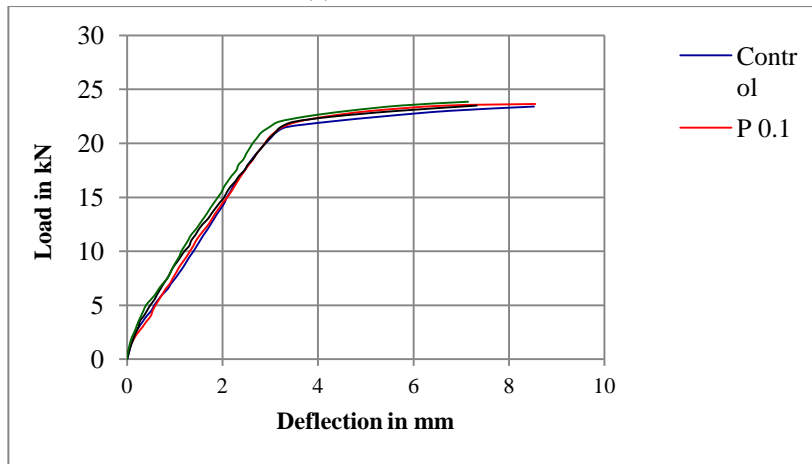
It was observed that beams reinforced with steel fibres have more ductile behavior than the control GPCC beam. It was noted that in the case of steel fibre reinforced geopolymer concrete beams, as the fibre content increases, the ductility also increases. The maximum value of the ductility factor is obtained for the beam with a fibre volume fraction of 0.5%. The ductility factor improves by 6%, 53% and 19% for volume fractions of 0.25%, 0.5% and 0.75% respectively. Beams reinforced with polypropylene fibres did not show any improvement in ductility when compared with control GPCC beam. In the case of glass fibre reinforced geopolymer concrete beams, ductility factor increases for all the volume fractions, however the maximum ductility was observed for the beam with a volume fraction of 0.01%. The improvement in ductility was found to be 48%, 7% and 13% for volume fractions of 0.01%, 0.02% and 0.03% respectively.

Table 5 Ductility factor

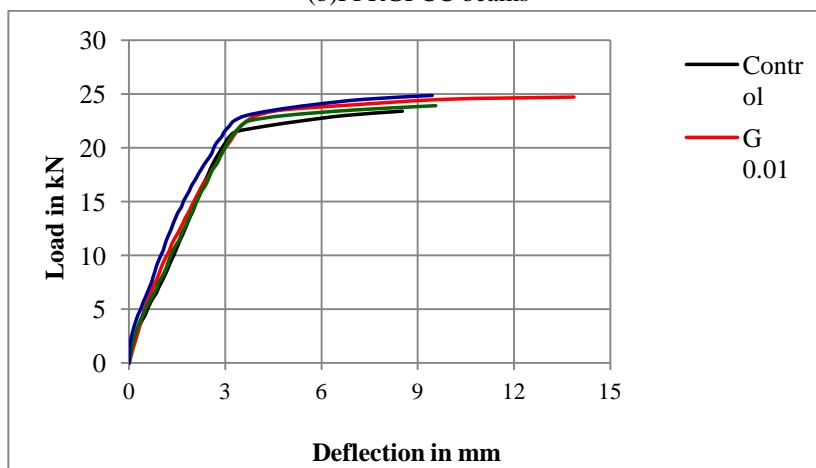
Beam ID	Deflection at ultimate load (δ_u) mm	Deflection at yield load (δ_y) mm	Ductility factor = δ_u / δ_y	
			Absolute	Relative
GPCC	8.52	3.34	2.55	1.00
S _{0.25}	10.3	3.82	2.70	1.06
S _{0.5}	14.14	3.63	3.90	1.53
S _{0.75}	12.98	4.29	3.03	1.19
P _{0.1}	8.55	3.25	2.39	0.94
P _{0.2}	7.32	3.21	2.28	0.89
P _{0.3}	7.14	2.98	2.40	0.94
G _{0.01}	13.87	3.68	3.77	1.48
G _{0.02}	9.56	3.49	2.74	1.07
G _{0.03}	9.45	3.27	2.89	1.13



(a)SFRGPCC beams



(b)PFRGPCC beams



(c)GFRGPCC beams

Fig. 4. Load-Deflection response

3.3 Load-Deflection response

The experimental load-deflection responses for all the tested beams are shown in Figs. 4 (a)-(c). All the beams followed the same pattern of load-deflection response. In general the load-deflection curve consisted of three regions, the first region is a linear region that indicates the response till the concrete cracks, the second region is also a linear region that shows the response till the steel reinforcement bar yields and the third region indicates the response after the yielding of steel reinforcement when there is an enormous rate of increase in deformation for subsequent application of loads. But it was not able to predict the first crack load exactly from the experimentally obtained load-deflection curve. Hence the first crack load was noticed only through the visual observation made during testing of beams.

3.4 Energy absorption capacity

The energy absorption capacity was found out by calculating the area under the load-deflection curve up to the ultimate load P_u and the calculated values are shown in Fig.5. The energy absorption capacities increased by 52%, 152% and 140% when steel fibres were added in volume fractions of 0.25%, 0.5% and 0.75% respectively when compared to GPCC specimen. The addition of polypropylene fibres did not show any increase in energy absorption capacity for the volume fractions of 0.2% and 0.3% whereas for a volume fraction of 0.1%, a slight increase in energy absorption capability in the order of 1.6% is noticed. When glass fibres were added, the maximum value of energy absorption is observed for a volume fraction of 0.01%. The increase in energy absorption capacity was found to be 89%, 19% and 16% for volume fractions of 0.01%, 0.02% and 0.03% respectively.

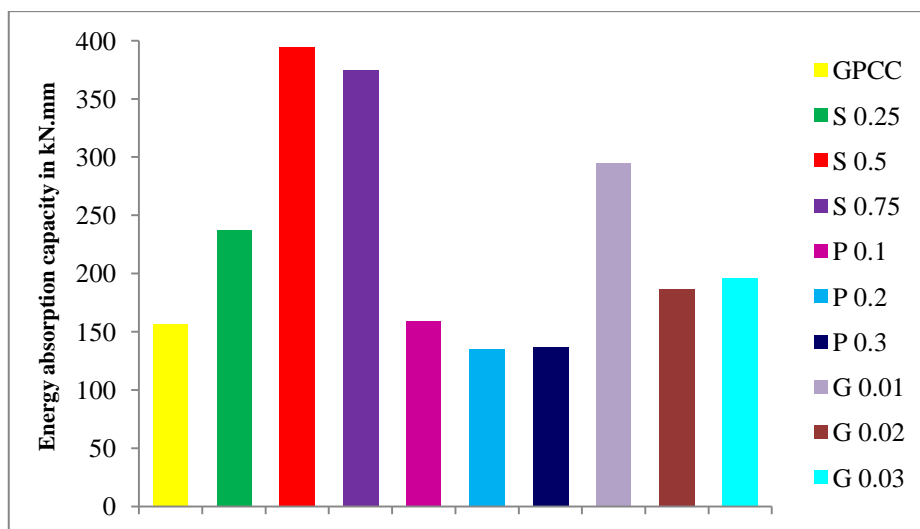


Fig.5 Energy absorption capacity

3.5 Failure modes

All the beams were tested experimentally for flexure by conducting two point loading tests. The failure pattern in the all the tested beams was observed as a flexure-shear failure. The beams showed initial cracking in the region of constant bending moment and further the cracks propagated in the vertical direction as the load was increased. At about 70 to 80 % of the ultimate load, shear cracks appeared near the supports and proceeded towards the compression zone. At the stage of ultimate failure, the shear cracks extended till the loading point and the crushing of concrete was noticed near the points of application of load. All the beams showed the same pattern of failure and the failure modes are shown in Figs. 6 (a)–(c).



(a) SFRGPCC beams



(b) PFRGPCC beams



(c) GFRGPCC beams

Fig. 6 Failure modes of beams

4. Analytical modeling using ANSYS

4.1 Geometry and modeling

The Finite Element Analysis included modeling of geopolymer composite reinforced concrete beams with the dimensions and properties corresponding to beams tested experimentally in the laboratory. The dimension of the full-size beam is 100 mm × 150 mm × 1000 mm. The span between the two supports is 900 mm. By taking the advantage of the symmetry of the beam and loading, one quarter of the full beam was used for finite element modeling. This approach reduces computational time and computer disk space requirements significantly.

4.2 Element types

Eight-noded solid brick elements (Solid 65) were used to model the concrete. This solid element has eight nodes with three degrees of freedom at each node – translations in x , y , and z directions. The element is capable of plastic deformation, cracking in three orthogonal directions, and crushing. Flexural and shear reinforcements were modeled as discrete reinforcement by using 3D spar elements (Link 8) as shown in Fig. 7(a). This element has two nodes with three degrees of freedom at each node – translations in x , y , and z directions. This element is also capable of plastic deformation. The fibre reinforcements were modeled as smeared reinforcements in the Solid 65 element as shown by red lines in each solid element in the Fig. 7(b). The total volume fraction and the material properties of the smeared reinforcements were defined according to the amount and the type of fibre reinforcements used. Properties of fibres include density, modulus of elasticity and yield stress.

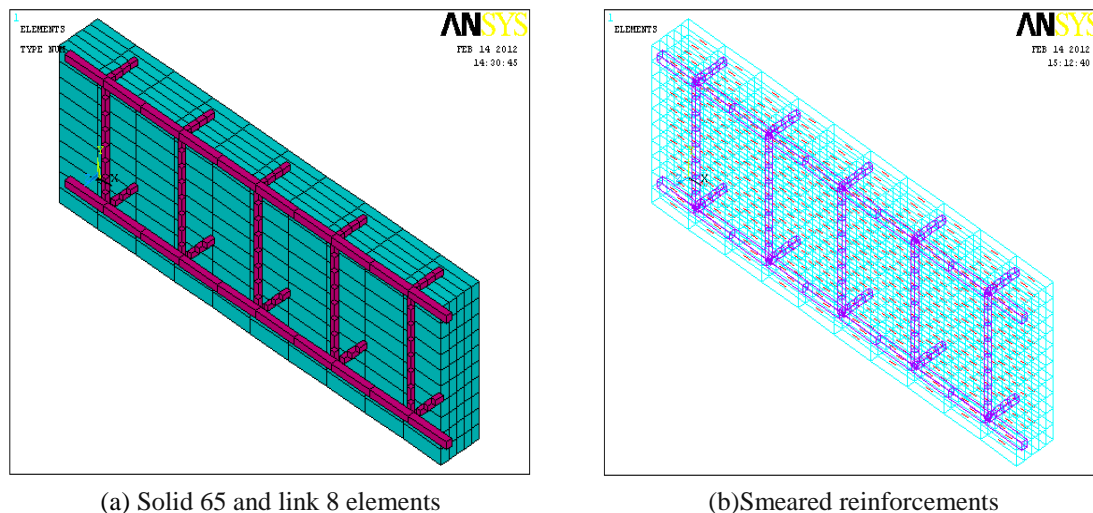


Fig. 7 Beam Model

4.3 Real constants

Real Constant Set 1 is used for the Solid65 element. For modeling the beam without fibre, a value of zero was entered for all real constants which turned off the smeared reinforcement capability of the Solid65 element. For modeling the beam with fibres, volume fraction of fibres, angle of orientation of fibres and material number for fibre reinforcement were entered. Real Constant Sets 2 and 3 are defined for the Link 8 element. Values for cross-sectional area and initial strain were entered. Cross-sectional area in set 2 refers to the main reinforcement. Cross-sectional area in set 3 refers to the shear reinforcement. A value of zero was entered for the initial strain as there is no initial stress in the reinforcement.

4.4 Material properties

Material model number 1 refers to the Solid 65 element. The Solid65 element requires linear isotropic and multi-linear isotropic material properties to properly model the concrete. The multi-linear isotropic material uses the von Mises failure criterion along with the William and Warnke model to define the failure of the concrete. The compressive uniaxial stress-strain relationship for the concrete model was obtained by using the equations given by MacGregor to compute the multilinear isotropic stress-strain curve for the concrete (Anthony, J. Wolanski 2004). For concrete, ANSYS requires input data for material properties as follows: Modulus of Elasticity, Poisson's ratio, Compressive uniaxial stress-strain relationship for concrete, ultimate uniaxial tensile strength (modulus of rupture) and the shear transfer coefficient β . The modulus of elasticity of the concrete was found out experimentally as 25330 MPa. Poissons ratio of concrete was assumed as 0.25 for all the models. The multilinear isotropic stress-strain implemented requires the first point of the curve to be defined by the user. It must satisfy Hooke's law as given by Eq. (1). The first point is taken as $0.3 f_c'$ which is in the linear range. Second, third and fourth points of the multilinear isotropic stress-strain curve were calculated from Eq.(2) with ε_o obtained from Eq. (3). Strains were selected and the stress was calculated for each strain. The last point is defined at f_c' . The multilinear stress strain values for concrete thus arrived are given in Table 6.

$$E_c = \frac{f}{\varepsilon} \quad (1)$$

$$f = \frac{E_c \varepsilon}{1 + \left(\frac{\varepsilon}{\varepsilon_o}\right)^2} \quad (2)$$

$$\varepsilon_o = \frac{2f_c'}{E_c} \quad (3)$$

where f = Stress at any strain ε
 ε = Strain at stress f

Table 6 Multilinear Isotropic stress- strain values

Compressive uniaxial stress-strain relationship	
Stress (MPa)	Strain
7.70	0.0003040
12.08	0.0005066
20.53	0.0010132
24.64	0.0015198
25.66	0.0020264

ϵ_o = Strain at the ultimate compressive strength f'_c

The ultimate tensile strength of concrete was found out experimentally as 3.48 MPa. The tensile strength of the fibre reinforced concrete varies according to the type of fibres and their volume fraction. The shear transfer coefficient β represents conditions of the crack face. The value of β ranges from 0 to 1.0, with 0 representing a smooth crack (complete loss of shear transfer) and 1.0 representing a rough crack (no loss of shear transfer). The value of β used in many studies of reinforced concrete structures, however, varied between 0.2 and 0.5. A number of preliminary investigations revealed that convergence problems were encountered at low loads with β value less than 0.2. Hence a value of 0.3 is adopted in this study for β . The required properties for steel reinforcing bars include modulus of elasticity, Poisson's ratio and yield strength. Yield strength of reinforcements was found out experimentally as 547 MPa by conducting tension tests on reinforcing bars. Poisson's ratio of steel was assumed as 0.3. Modulus of elasticity of steel was taken as 2×10^5 MPa.

4.5 Meshing

To obtain satisfactory results from the Solid 65 element, a rectangular mesh is recommended. Therefore, the mesh was setup such that rectangular elements were created. Each concrete mesh element is a prism of size $50 \times 10 \times 15$ mm. In this investigation, the technique that was used to model the steel reinforcement is the discrete model. The reinforcement in the discrete model uses 3D spar or link elements that are connected to the nodes of the concrete mesh. Hence, the concrete and the reinforcement mesh share the same nodes and concrete occupies the same regions occupied by the reinforcement. However, the necessary mesh attributes as described in Table 7 were set before meshing of the model is done.

4.6 Loads and boundary conditions

In order to get a unique solution displacement boundary conditions are needed to constrain the model. To ensure that the model acts the same way as the experimental beam, boundary conditions need to be applied at points of symmetry, and where the supports exist. The symmetry boundary conditions were set first. The model that was used is symmetric about two planes. Nodes defining a vertical plane through the centroid of the beam cross-section define a plane of symmetry. To model the symmetry, nodes on this plane must be restrained in the perpendicular direction. These nodes (at $X = 500$) therefore, have a degree of freedom constraint $U_x = 0$. Secondly, all nodes selected at $Z = 0$ define another plane of symmetry. These nodes were given the constraint $U_z = 0$.

Table 7 Mesh attributes for the model

Model parts	Element type	Material number	Real constant set
Concrete beam	1	1	1
Main reinforcement	2	2	2
Shear reinforcement	2	3	3

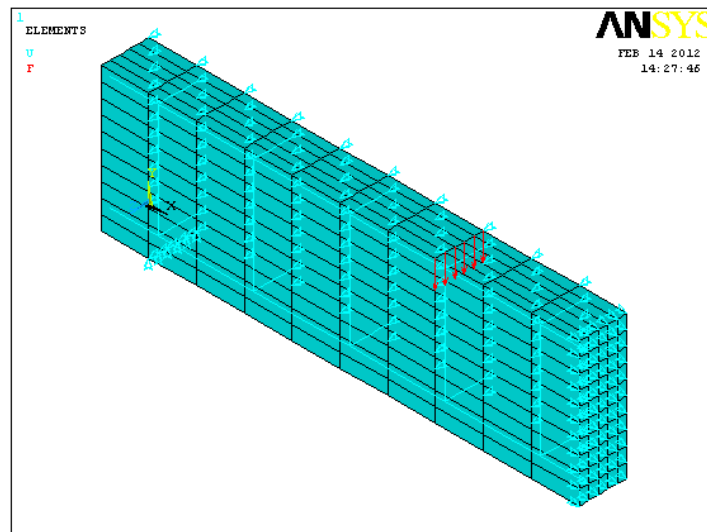


Fig.8. Loads and boundary conditions

The support was modeled such that a roller was created. A single line of nodes along the Z direction (at $X = 50$ and $Y = 0$) were given constraint in the U_y , and U_z directions, applied as constant values of 0. By doing this, the beam will be allowed to rotate at the support. The load applied at each node of one quarter model is $1/12^{\text{th}}$ of the actual load applied in the beam. The loads and boundary conditions applied to the model are shown in Fig.8.

4.7 Nonlinear solution

In nonlinear analysis, the total load applied to a finite element model is divided into a series of load increments called load steps. After the completion of each incremental solution, the stiffness matrix of the model is adjusted to reflect nonlinear changes in the structural stiffness before proceeding to the next load increment. The Newton–Raphson equilibrium iterations were used in the nonlinear solutions for updating the model stiffness. Before each solution, the Newton–Raphson approach assesses the out-of-balance load vector, which is the difference between the restoring forces (the loads corresponding to the element stresses) and the applied loads. Then, the program carries out a linear solution using the out-of-balance loads and checks for convergence. If convergence criteria are not satisfied, the out-of-balance load vector is re-evaluated, the stiffness matrix is updated, and a new solution is carried out. This iterative procedure continues until the

results converge. In this study, convergence criteria for the reinforced concrete solid elements were based on force and displacement, and the convergence tolerance limits were set as 0.1 for both force and displacement in order to obtain the convergence of the solutions. For the nonlinear analysis, automatic time stepping in the ANSYS program predicts and controls the load step sizes. Based on the previous solution history and the physics of the models, if the convergence behaviour is smooth, automatic time stepping will increase the load increment upto the given maximum load step size. If the convergence behavior is abrupt, automatic time stepping will divide the load increment until it is equal to a selected minimum load step size. The maximum and minimum load step sizes are required for the automatic time stepping. The total load is to be divided into number of suitable load steps (load increments) by conducting a few trial analyses until a smooth load versus deflection curve is obtained.

5. Finite element analysis results

5.1 Behaviour at first cracking

The analysis based on the design for flexure given by Macgregor (1992) for a reinforced concrete beam was used in the present study to compare with the finite element analysis results in the linear region. The first crack load was determined theoretically based on the theory given by Macgregor. Once cracking occurs, it becomes more difficult to predict deflections and stresses. Therefore the stresses in concrete were found out theoretically for all the beams at the first crack load predicted by ANSYS. The load, deflection and the extreme fibre stress in concrete at the first crack predicted by the ANSYS model were compared with the theoretical hand calculated results and are given in Table 8. It can be seen that the analytical and theoretical results were in good agreement with each other for all the cases.

Table 8 Comparison of analytical and theoretical results

Beam ID	Analytical			Theoretical		
	First crack load kN	Deflection mm	Extreme fibre stress in concrete MPa	First crack load kN	Deflection mm	Extreme fibre stress in concrete MPa
GPCC	5.353	0.17	3.65	4.899	0.16	3.80
S _{0.25}	5.586	0.18	3.41	5.040	0.17	3.97
S _{0.5}	7.288	0.23	4.86	6.476	0.22	5.18
S _{0.75}	7.969	0.25	5.25	6.983	0.23	5.66
P _{0.1}	5.928	0.19	4.07	5.434	0.18	4.21
P _{0.2}	6.147	0.20	4.22	5.631	0.19	4.37
P _{0.3}	6.783	0.22	4.64	6.223	0.21	4.82
G _{0.01}	5.300	0.17	3.61	4.843	0.16	3.76
G _{0.02}	4.766	0.15	3.27	4.364	0.15	3.39
G _{0.03}	6.287	0.20	4.31	5.744	0.19	4.47

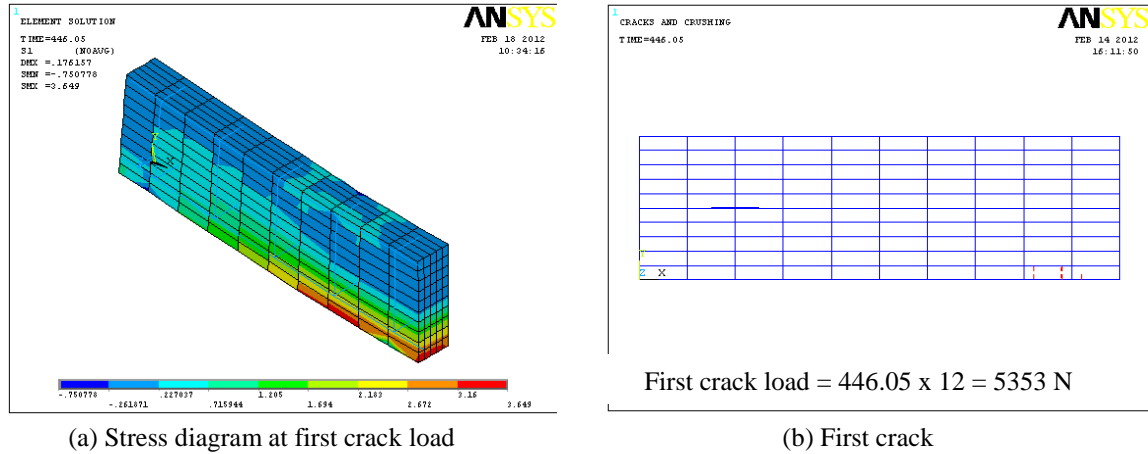


Fig.9 GPCC beam

The initial cracking of the GPCC beam in the finite element model corresponds to a load of 5.353 kN that creates stress just beyond the modulus of rupture of concrete (3.48MPa). The stress increases upto 3.65 MPa when the first crack occurs as shown in Fig.9 (a). The first crack occurs in the constant moment region and it is a flexural crack. The first crack in the finite element model appears as red circles and the first crack formed in GPCC beam is shown in Fig.9 (b).

5.2 Behaviour at first cracking

In the non-linear region of the response, further cracking of the beams occur as more loads are applied. Cracks grow in the region where there is a constant moment and the beams started cracking out towards the supports. Significant flexural cracking occurs and subsequently diagonal tension cracks also appear in the model. This type of behavior is observed for all the beams. For the GPCC beam, yielding of steel reinforcement occurs at a load of 22.64 kN. At this point, the displacements of the beam started to increase at a higher rate as more loads are applied. The moment of inertia of the cracked section, yielding of steel reinforcement and nonlinear behaviour of concrete now defines the flexural rigidity of the beam members. The ability of the beam to distribute the load throughout the cross section has diminished greatly. Therefore a higher value of deflections occurs at the centerline of the beam.

5.3 Strength limit state

For the GPCC beam, at a load of 23.68 kN, the beam can no longer support additional load as indicated by an impossible convergence failure. Severe cracking occurs throughout the entire constant moment region and the cracks have reached the top of the beam. It was also noticed that before the collapse of the beam, a few compressive cracks appear at the upper part of the beam due to crushing failure of the concrete as indicated by the red circles in ANSYS which is shown in Fig.10.

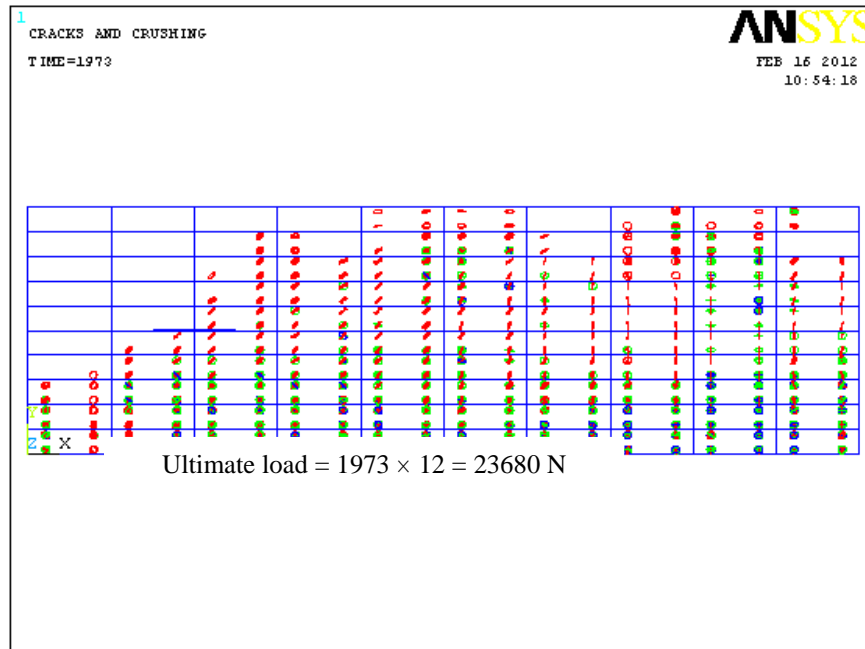


Fig. 10 Failure of GPCC beam

5.4 Strength limit state

The first crack loads and the ultimate loads for control and fibre reinforced geopolymer concrete beams predicted by finite element analysis using ANSYS were compared with the experimental results as shown in Table 9. It was found that a good correlation was obtained between the experimental results and those obtained from ANSYS. It can be seen that the finite element model predicts the behaviour of beams well with good accuracy. The mid span deflections at the ultimate load recorded in the experiments were compared with the deflections obtained using finite element analysis and it was found that they were in good agreement with each other as shown in Table 10. The load-deflection responses recorded by the finite element model were compared to the experimental results where good concurrence has been achieved. A comparison between the load-deflection curves obtained from ANSYS and experiments for all the ten beams are shown in Figs. 11 to 14. Thus the analytical model developed using ANSYS has shown to provide accurate prediction of the load-deflection behaviour of GPCC and fibre reinforced GPCC beams. The slight deviations in the load-deflection curves may be due to the following reasons. In the experimentally tested beams micro cracks may be present that could be produced by drying shrinkage in the concrete whereas the finite element model does not include the effect of micro cracks. The second reason is that, in the finite element analysis, perfect bonding is assumed between the concrete and the steel reinforcement, but the same assumption would not be true for the experimentally tested beam.

Table 9 Comparison of first crack and ultimate loads

Beam ID	First crack load kN		Ultimate Load (P_u) kN		$P_{u,A}/P_{u,E}$
	Experimental	Analytical	Experimental	Analytical	
GPCC	5.15	5.353	23.40	23.68	1.01
S _{0.25}	5.30	5.586	27.60	27.81	1.01
S _{0.5}	6.85	7.288	31.85	32.09	1.01
S _{0.75}	7.55	7.969	34.50	35.77	1.04
P _{0.1}	5.80	5.928	23.65	23.96	1.01
P _{0.2}	5.95	6.147	23.50	24.02	1.02
P _{0.3}	6.45	6.783	23.85	24.31	1.02
G _{0.01}	5.10	5.300	24.70	24.84	1.01
G _{0.02}	4.50	4.766	23.90	24.73	1.04
G _{0.03}	6.00	6.287	24.87	25.26	1.02

Table 10 Comparison of mid span deflection

Beam ID	Mid span deflection mm		$\delta_{u,anal} / \delta_{u,exp}$
	Experimental	Analytical	
GPCC	8.52	8.94	1.05
S _{0.25}	10.3	11.29	1.10
S _{0.5}	14.14	14.31	1.01
S _{0.75}	12.98	13.33	1.03
P _{0.1}	8.55	8.73	1.02
P _{0.2}	7.32	7.47	1.02
P _{0.3}	7.14	7.93	1.11
G _{0.01}	13.87	14.43	1.04
G _{0.02}	9.56	9.75	1.02
G _{0.03}	9.45	9.64	1.02

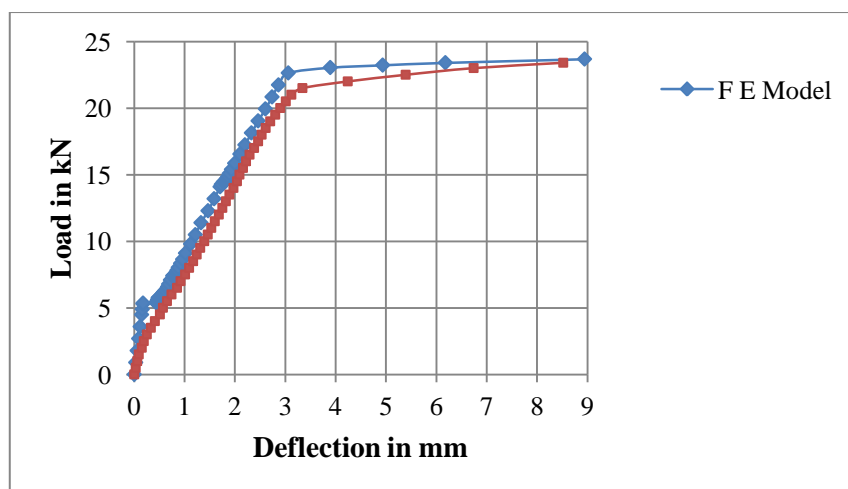
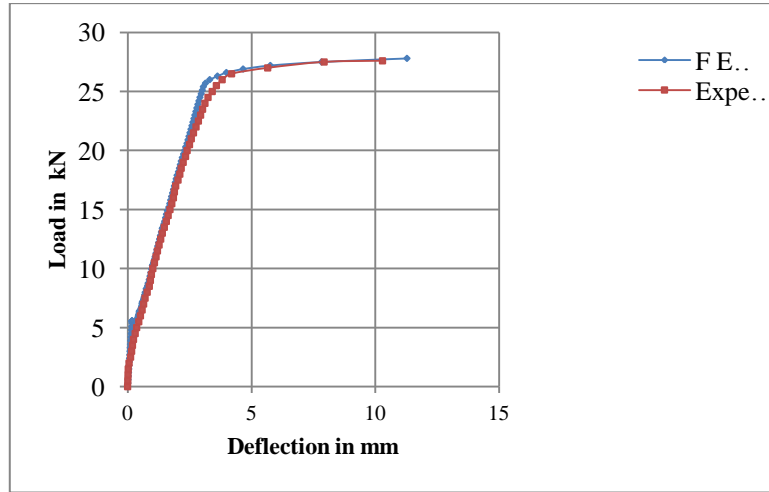
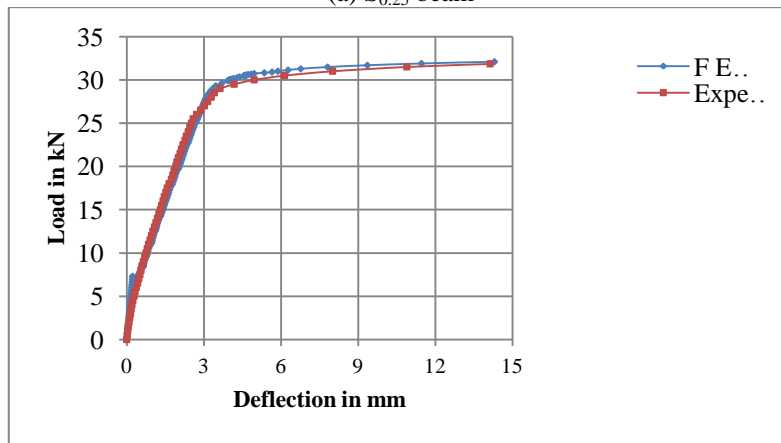


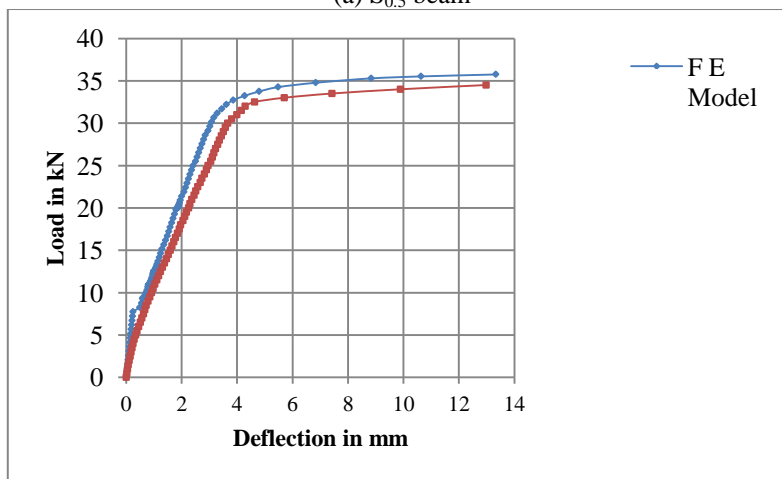
Fig. 11 Experimental Vs FEM load deflection response-GPCC beam



(a) $S_{0.25}$ beam

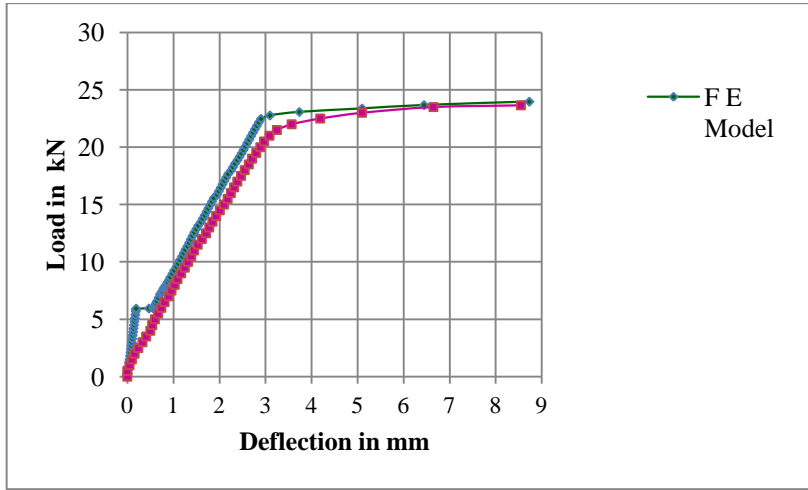


(a) $S_{0.5}$ beam

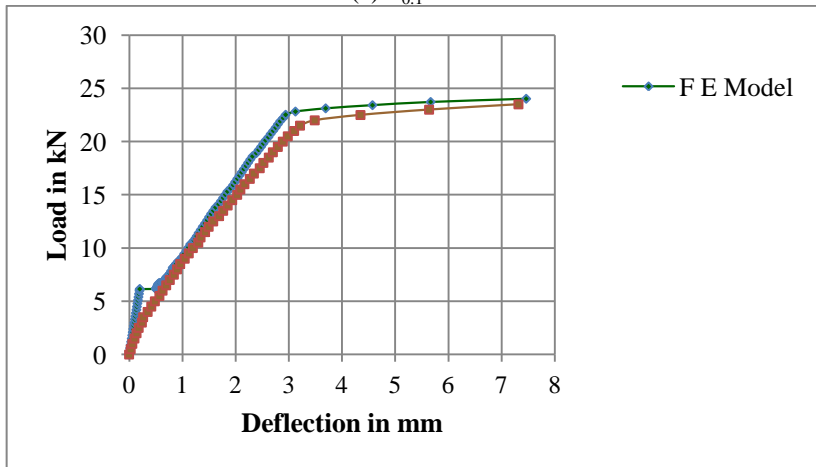


(a) $S_{0.75}$ beam

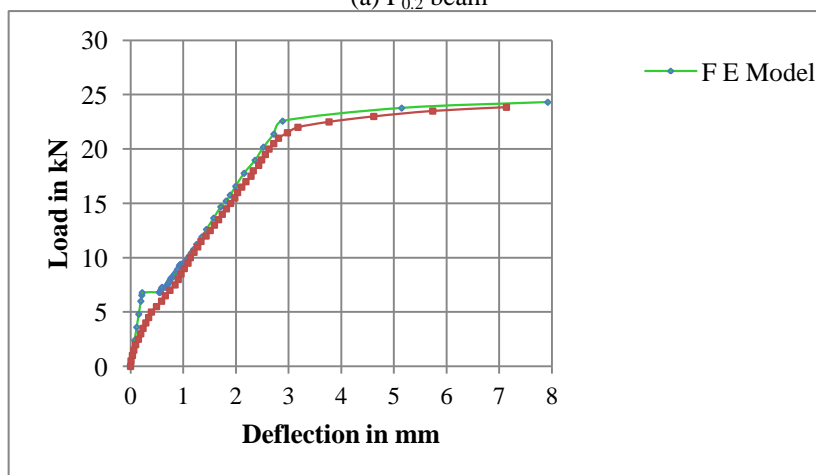
Fig. 12 Experimental Vs FEM load deflection response-SFRGPCC beam



(a) P_{0.1} beam

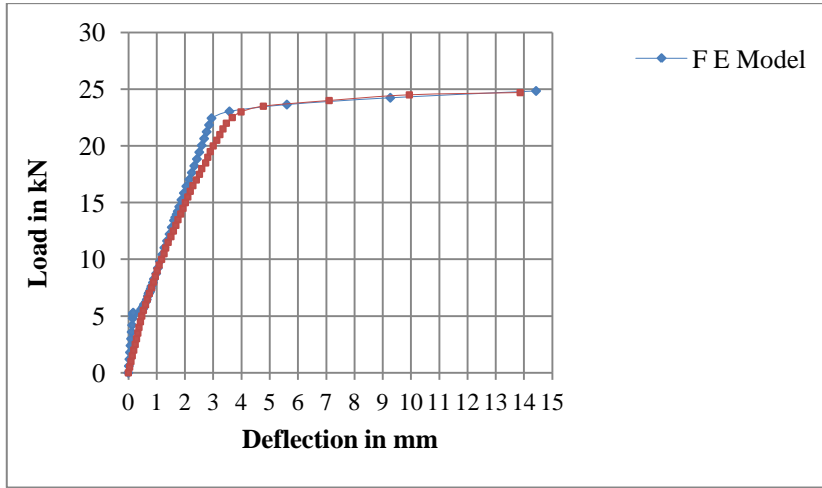


(a) P_{0.2} beam

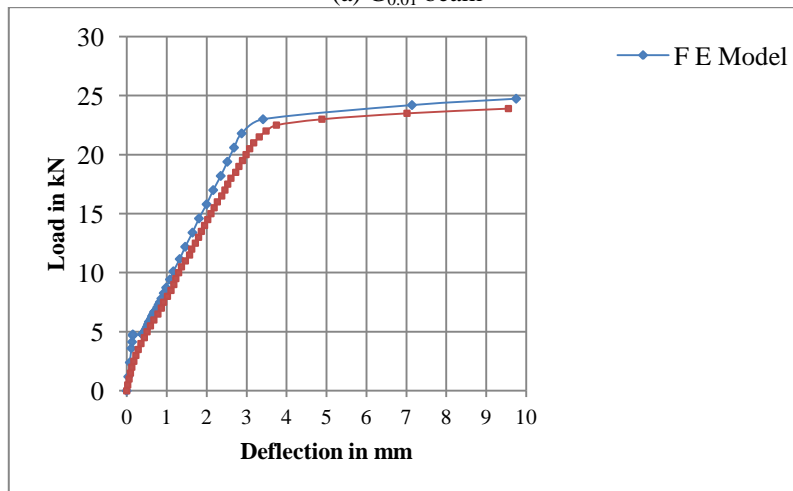


(a) P_{0.3} beam

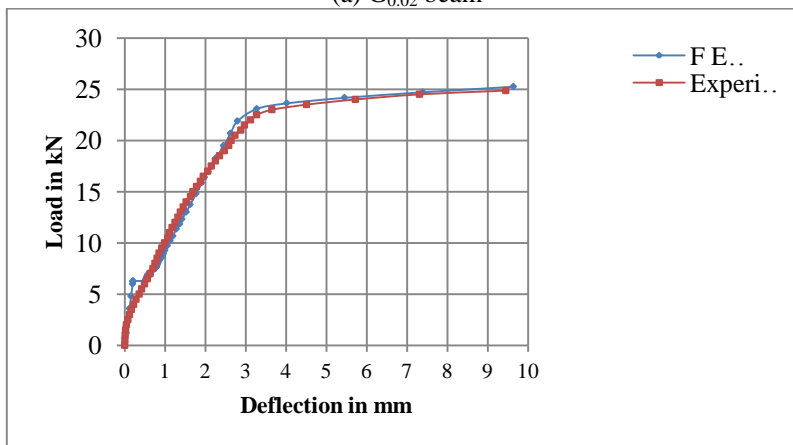
Fig. 13 Experimental Vs FEM load deflection response-PFRGPCC beam



(a) G_{0.01} beam



(a) G_{0.02} beam



(a) G_{0.03} beam

Fig. 14 Experimental Vs FEM load deflection response-GFRGPCC beam

6. Conclusions

Based on the results obtained in this investigation, the following conclusions are drawn:

- In case of SFRGPCC beams, the first crack load and the ultimate load increase as the volume fraction of steel fibres increases. The gain in ultimate load carrying capacity is more significant in the case of SFRGPCC beams due to the addition of fibres. When compared to GPCC beams, the ultimate load increases by 18%, 36% and 47% for 0.25%, 0.5% and 0.75% of steel fibres respectively. For steel fibre reinforced geopolymer concrete composite beams, as the fibre content increases, the ductility also increases. The maximum value of the ductility factor is obtained for the beam with a fibre volume fraction of 0.5%. The ductility factor improves by 6%, 53% and 19% for volume fractions of 0.25%, 0.5% and 0.75% respectively. The energy absorption capacities increased by 52%, 152% and 140% when steel fibres were added in volume fractions of 0.25%, 0.5% and 0.75% respectively.

- Due to the addition of polypropylene fibres, the increase in ultimate load is very marginal as compared to control GPCC beam. The increase in load carrying capacity is only in the order of 2% even for a volume fraction of 0.3%. Beams reinforced with polypropylene fibres did not show any improvement in ductility when compared with control GPCC beam. The addition of polypropylene fibres did not show any increase in energy absorption capacity for the volume fractions of 0.2% and 0.3% whereas for a volume fraction of 0.1%, a slight increase in energy absorption capability in the order of 1.6% is noticed.

- In case of GFRGPCC beams, the increase in ultimate load carrying capacity was not that much significant when compared to control GPCC beam. The ultimate load increases by only about 6%, 2% and 6% for 0.01%, 0.02% and 0.03% of glass fibres respectively. In the case of glass fibre reinforced geopolymer concrete beams, ductility factor increases for all the volume fractions, however the maximum ductility was observed for the beam with a volume fraction of 0.01%. The improvement in ductility was found to be 48%, 7% and 13% for volume fractions of 0.01%, 0.02% and 0.03% respectively. When glass fibres were added, the maximum value of energy absorption is observed for a volume fraction of 0.01%. The increase in energy absorption capacity was found to be 89%, 19% and 16% for volume fractions of 0.01%, 0.02% and 0.03% respectively.

- The load, deflection and the extreme fibre stress in concrete at the first crack predicted by the ANSYS model were compared with the theoretical hand calculated results. It can be seen that the analytical and theoretical results were in good agreement with each other for all the cases.

- The failure mechanism of GPCC beam and fibre reinforced GPCC beams were modeled quite well using finite element software ANSYS and the failure loads predicted were found to be very close to the failure load measured during experimental testing. The first crack loads, ultimate loads and the mid span deflections for control and fibre reinforced geopolymer concrete composite beams predicted by finite element analysis were compared with the experimental results and it was found that a good correlation was obtained between the experimental results and those obtained from ANSYS. It can also be seen that the finite element model predicts the behaviour of beams well. The load-deflection behaviour of GPCC and fibre reinforced GPCC beams obtained from the analytical models developed using ANSYS were found to be closer with that obtained from experiments.

- In case of mass production, the cost of geopolymer concrete is same as that of OPC concrete besides environmental benefits in terms of reduction of CO₂ emissions without any compromise in their properties.

References

- Amol, A.P., Chore, H.S. and Dode, P.A. (2014), "Effect of curing condition on strength of geopolymer concrete", *Adv. Concr. Constr.*, **2**(1), 29-37.
- Anthony J.W. (2004), "Flexural behavior of reinforced and prestressed concrete beams using finite element analysis", M.S Thesis, Faculty of the Graduate School, Marquette University, Milwaukee, Wisconsin.
- Anuar, K.A., Ridzuan, A.R.M. and Ismail, S. (2011), "Strength characteristic of geopolymer concrete containing recycled concrete aggregate", *Int. J. Civil Environ. Eng.*, **11**(1), 81-85.
- Anurag Mishra, Deepika Chodhary, Namrata Jain, Manish Kumar, Nidhi Sharda and Durga Dutt. (2008), "Effect of concentration of alkaline liquid and curing time on strength and water absorption of geopolymer concrete", *ARPJ. Eng. Sci.*, **3**(1), 14-18.
- Davidovits, J. (1999), "Chemistry of Geopolymeric Systems, Terminology", *Geopolymer '99 International Conference*, France.
- Ganesan, N., Indira, P.V. and Anjana Santhakumar. (2013), "Engineering properties of steel fibre reinforced geopolymer concrete", *Adv. Concr. Constr.*, **1**(4), 305-318.
- Malhotra, V.M. (2002), "High-performance high-volume fly ash concrete", *ACI Concr. Int.*, **24**(7), 1-5.
- Malhotra, V.M. (2002), "Introduction: Sustainable Development and Concrete Technology", *ACI Concrete International*, **24**(7), 22.
- Monita Olivia and Hamid R. Nikraz. (2011), "Strength and water penetrability of fly ash geopolymer concrete", *ARPJ. Eng. Appl. Sci.*, **6**(7), 70-78.
- Roy, D.M. (1999), "Alkali-activated cements, opportunities and challenges", *Cement and Concrete Research*, **29**(2), 2249-54.
- Siva Konda Reddy, B., Vara Prasad, J. and Naveen Kumar Reddy, K. (2010), "Strength and workability of low lime fly ash based geopolymer concrete", *Indian J. Sci. Tech.*, **3**(12), 1188-1189.
- Song, X.J., Marosszeky, M., Brungs, M. and Munn, R. (2005), "Durability of fly ash based geopolymer concrete against sulphuric acid attack", *Proceedings of the International Conference on durability of building materials and components*, LYON, France.
- Vijaya Rangan, B, Dody Sumajouw, Steenie Wallah, Djwantoro Hardjito.(2006), "Studies on reinforced low – calcium fly ash –based geopolymer concrete beams and columns", *International Conference on Pozzolana Concrete and Geopolymer*, Khon Kaen, Thailand, May.
- Vijaya Rangan, B. (2008), *Fly Ash Based Geopolymer Concrete*, Research report GC4, Curtin University of Technology, Perth, Australia.
- Wallah, S.E. and Rangan, B.V. (2006), "Low-calcium fly ash-based geopolymer concrete: Long-term properties", *Research Report GC 2 Engineering Faculty in Curtin University of Technology*, Perth, Australia.